Reductive dissolution of natural jarosite in a tidally inundated acid sulfate soil: geochemical implications

Annabelle Keene[A], Scott Johnston[A], Richard Bush[A], Leigh Sullivan[A] and Ed Burton[A]

[A]Southern Cross GeoScience, Southern Cross University, Lismore, NSW, Australia, Email annabelle.keene@scu.edu.au

Abstract
Jarositic pedofeatures are a significant mineralogical indicator of the weathering conditions in ASS wetland environments. The geochemical processes in the reductive dissolution of natural jarosite are presented for a tidally inundated acid sulfate soil (ASS) of northeastern Australia. The extent of reductive dissolution of jarosite was determined from mineral micromorphology and by identifying differences in geochemical weathering along a toposequence. With increasing pH and decreasing Eh under tidal inundation, reduction of Fe(III) minerals occurred and jarosite became increasingly unstable. Direct evidence from scanning electron microscopy (SEM) and x-ray diffractometry (XRD) identified mineral structure and composition consistent with jarosite. Natural jarosite from the intertidal zone exhibited features associated with dissolution. Molar ratios of Fe to K indicated increasing depletion of K in natural jarosite downslope. Results provide important insights to the observed and predicted variability and stability of jarosite with tidal inundation.

Key Words
K-jarosite, coastal ASS, elemental composition, seawater inundation, remediation, East Trinity.

Introduction

The ferric sulfate mineral jarosite ($KFe_3(SO_4)_2(OH)_6$) is formed from pyrite oxidation and precipitates as pore fillings and coatings in soils under strongly oxidising and acidic conditions. Its presence is commonly observed as pale yellow mottles (Munsell soil colour 2.5Y 6/8) in the sulfuric horizon of acid sulfate soils (ASS). Natural jarosite crystals exhibit a classic euhedral ortho-rhomboidal morphology, with K, Na and H_3O^+ combining in the alkali position of the lattice structure (Brophy and Sheridan 1965). While the compositional variability of jarosite in ASS has not been published extensively, K-jarosite has been reported as the most abundant form (van Breemen 1973). In addition, the elemental composition of jarosite can provide an indication of the antecedent soil porewater conditions, and hence reflect the environment of precipitation (Dutrizac 1983). The substitution of Na into the lattice structure indicates increasing reactivity and solubility of jarosite, as jarosite rich in Na is considered less stable than K-jarosite (Gasharova *et al.* 2005). Jarosite is considered stable only under relatively oxidised (Eh >400 mV) and acid (pH 2 to 4) conditions. At higher pH values, jarosite is metastable with respect to goethite and slowly hydrolyses to fine-grained iron oxide, FeOOH. Hydrolysis is generally enhanced by leaching and by supply of bases.

It is well established that the metastable Fe(III) oxides which form in sulfuric horizons are prone to reductive dissolution when subjected to reducing conditions. This can lead to large increases in Fe^{2+} and concomitant increases in pH (e.g. van Breemen and Harmsen 1975). However, to our knowledge, there are few field-based studies in coastal ASS landscapes specifically examining the reductive dissolution of jarosite. This study will contribute to the present knowledge of jarosite behaviour by examining the mineralogical variability with tidal inundation in ASS. This has important implications for environmental rehabilitation and management of these coastal ASS landscapes.

Methods

Study site

The study site was located in a Holocene sedimentary coastal plain at East Trinity near Cairns in northeastern Australia (145°48′ E, 16°56′ S), and covers an area of 940 ha. It experiences a tropical monsoonal climate with summer-dominant rainfall and a maximum tidal range in Trinity Inlet of around 3.2 m. Extensive drainage and clearing of vegetation for agriculture in the early 1970s caused oxidation of pyrite-rich, estuarine sediments and subsequent development of severely acidic soils. Various parts of the site have undergone remediation from 2001, which consisted of the reintroduction of regular tidal inundation to the previously drained ASS (Johnston *et al.* 2009a; Powell and Martens 2005). For this study, sampling sites were located along an established transect in the upper reaches of Firewood Creek sub-catchment and selected to represent a topographic sequence spanning the supratidal to intertidal zones (0.6-0.0 m AHD).

The transect was located upstream from the tidal floodgates and has experienced regular but attenuated tidal inundation for the preceding 5 years (i.e. since 2003).

Soil collection and handling
Four duplicate cores were collected at selected distances (20, 40, 60, 80 and 100 m) along the transect. Soil descriptions (texture, colour, etc.) were undertaken in the field for stratigraphy (see Figure 3a). Soils and sediments were rapidly sectioned into specified depth intervals (from 0–0.05, 0.05–0.15 m depth, and thereafter in 0.10 m increments) to a depth of at least 1.25 m for analysis of the solid fraction. Field measurements of pH (pH_F) and Eh (Eh_F) were made immediately on duplicate cores by direct probe insertion using calibrated Intermediate Junction Ag/AgCl combination pH and ORP electrodes with a saturated KCl reference solution. Eh measurements were corrected to the Standard Hydrogen Electrode (SHE). Samples from the equivalent depth intervals were bulked and placed into air-tight, sealable polyethylene bags, completely filled with material (i.e. no enclosed air). All soil and sediment samples were stored frozen until analysis to minimise possible oxidation of reduced species. Soil porewaters were also sampled at selected distances along the transect using a peeper equilibration dialysis method. Measurements of pH and Eh were made immediately using calibrated electrodes. Jarositic pedofeatures were collected from the sulfuric horizon (0.20-0.50 m depth) at corresponding distances. Samples were dried in a N_2 atmosphere at 20 °C, and jarositic pedofeatures were carefully removed by hand, minimising the inclusion of clay material and organic matter. These fragments were stored separately in air-tight plastic vials for morphological characterisation. A portion of the resultant samples were prepared for mineralogical and geochemical analysis by gently grinding and sieving to <63 μm, then stored in air-tight plastic vials.

Geochemical analyses
Frozen samples were thawed under N_2 and homogenised with a spatula for geochemical analysis of the solid fraction. Gravimetric moisture content (θg) was determined by oven-drying sub-samples at 105 °C until a constant mass. A portion of soil samples were oven-dried at 85 °C for at least 24 h and gently ground. Aqueous extractions were undertaken in duplicate on 2 g oven-dry soil using a 1:5 soil to water ratio. Water-soluble cations (Na^+, K^+, Ca^{2+}, Mg^{2+} and Fe^{2+}) and anions (SO_4^{2-}) were determined in filtered (0.45 μm) aqueous extracts using Inductively Coupled Plasma-Optical Emission Spectrometry (ICP-OES; Perkin-Elmer DV4300). Water soluble Cl^- was also determined in aqueous extracts using flow injection analysis (FIA; Lachat QuikChem 8000). Total C was determined gravimetrically on oven-dry materials using a LECO CNS-2000 Carbon, Nitrogen and Sulfur Analyzer. Near-total Fe and S were determined on oven-dry materials by hot aqua-regia digestion (3:1 HCl:HNO_3, 95 °C, 1 h) using Inductively Coupled Plasma-Mass Spectrometry (ICP-MS; Perkin-Elmer Optima ELAN-DRCe).

Mineralogical analyses
The mineralogical composition of the dried jarositic pedofeatures was identified by X-ray powder diffraction (XRD). The diffractograms were obtained with a Bruker D4-Endeavor diffractometer, with a 2.2 kW CoK radiation source and a Lynx Eye detector. The diffractograms were comprised of randomly oriented aggregates of the mineral fraction. Samples were scanned stepwise from 15° to 80° 2θ using 0.05° steps and a 4 s count time. Scanning electron microscopy (SEM) and elemental analysis (energy dispersive X-ray, EDX) of jarositic pedofeatures were carried out with a Leica 440. Material was carefully sampled from pedofeatures under a light microscope, then mounted on aluminium stubs and coated in carbon. Microanalysis was carried out after internal calibration with an OXFORD microprobe ISIS system.

Results
Prior to re-establishing tidal inundation, soils along the toposequence were described as having distinct sulfuric horizons in the upper 1 m with pedofeatures typical of ASS, including jarosite and Fe(III) oxides mottles (Johnston *et al.* 2009b). Following regular tidal inundation over 5 years, ASS materials were transformed from Hydraquentic Sulfaquepts to Typic Sulfaquents (Johnston *et al.* 2009b). Soil geochemical characteristics of the former mineral sulfuric horizon (0.10–0.70 m depth; GBj) are shown in Table 1. Reducing conditions were evident in the lower intertidal zone (i.e. at lower elevation), and these soils were characterised by greater concentrations of soluble Na^+ and Cl^-, reflecting seawater influence, and increasing soluble K^+ contents. The abundance, size and prominence of jarosite mottles were lower in the intertidal ASS compared with the supratidal ASS. This is consistent with circumneutral pH and moderately reducing Eh, indicating that the geochemical conditions for the intertidal ASS lie outside the stability field for jarosite (Table 1, Figure 1).

Table 1. Soil geochemical characteristics of the mineral sulfuric horizon (0.10–0.70 m depth) along the toposequence examined in this study. Data shown is the mean of n=7 depth intervals.

Zone	Supratidal	Supratidal	Intertidal	Intertidal	Intertidal
Distance (m)	20	40	60	80	100
Field pH_F	4.5	4.2	5.4	6.1	6.1
Field Eh_F (mV)	589	517	217	103	143
Soluble Cl^- (mmol/kg)	65	107	251	444	451
Soluble SO_4^{2-} (mmol/kg)	20	21	19	11	11
Soluble Na^+ (mmol/kg)	7	12	27	45	48
Soluble K^+ (mmol/kg)	1.2	1.4	1.9	2.7	2.8
Soluble Fe^{2+} (mmol/kg)	0.31	0.30	0.64	0.06	0.06
Total Fe (mmol/kg)	487	493	600	410	330
Total S (mmol/kg)	282	369	337	171	126

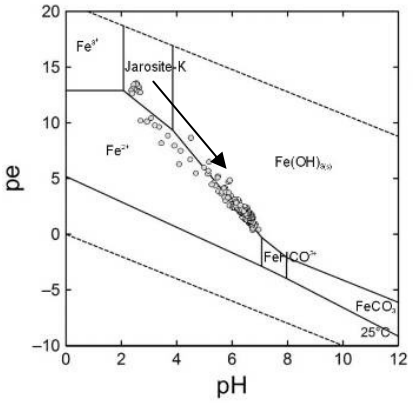

Figure 1. pE-pH diagram for tidally inundated ASS, based on porewater pH and Eh along the toposequence. Stability fields of Fe species are shown. Direction of arrow indicates increasing tidal inundation (i.e. with lower elevation).

The pe-pH diagram (Figure 1) describes the geochemical conditions for various stable Fe mineral phases. Porewater pH and Eh were shown to lie close to the Fe(II)/Fe(III) boundary (Figure 1), suggesting that the reduction of Fe(III) minerals is controlling soil geochemical conditions with increasing tidal inundation. Various Fe(III) oxide minerals (including ferrihydrite, schwertmannite and goethite) that form in ASS sulfuric horizons have been shown to undergo reductive dissolution after reflooding (e.g. van Breemen and Harmsen 1975). Under increasing pH and decreasing Eh conditions typical of tidally inundated ASS, jarosite is increasingly unstable (Figure 1).

The natural yellow precipitates from the former sulfuric horizon along the toposequence were identified as jarosite from X-ray diffractograms (Figure 2a). Crystal morphologies evident from scanning electron photomicrographs were consistent with jarosite, and exhibited a classic euhedral ortho-rhomboidal form (Figure 2b, c). Figure 2b shows that jarosite from the supratidal zone (i.e. at 20 m upslope on transect) was generally inter-grown euhedral crystals >1 μm with clearly defined edges and planar surface features. In contrast, jarosite from the intertidal zone (i.e. at 100 m downslope on transect) exhibited features consistent with dissolution, including smaller, sub-rounded crystals with clearly visible etch pits (Figure 2c).

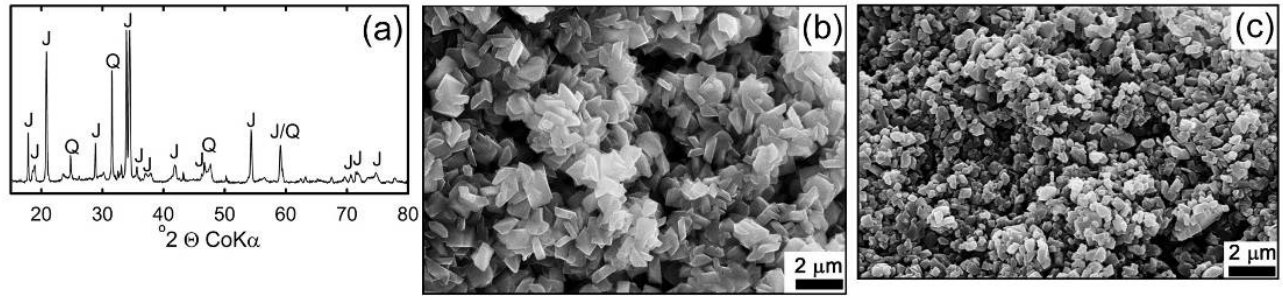

Figure 2. Representative X-ray diffractogram of jarositic pedofeatures (a), and scanning electron photomicrographs of natural jarosite from 20 m (supratidal zone) (b) and 100 m (intertidal zone) (c) along the toposequence.

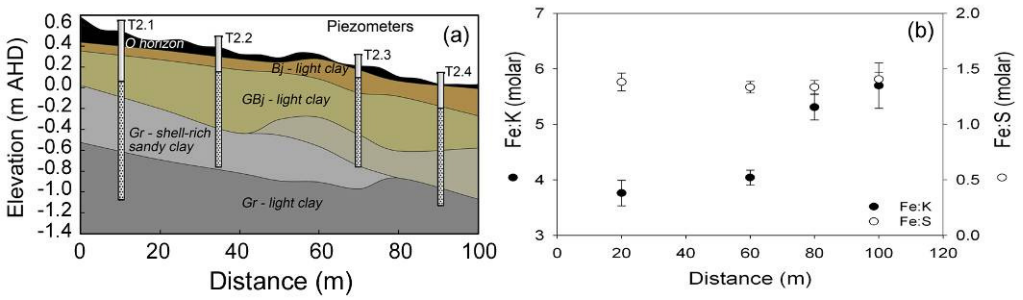

Figure 3. Stratigraphic cross-sectional profile along the toposequence (a). Horizon boundaries are described after Dent (1986). Relationship between elemental composition of jarosite from SEM-EDX and distance (m) (b). Molar ratios of Fe:K and Fe:S (± standard deviation) are shown.

The elemental composition of the jarositic pedofeatures was confirmed by SEM-EDX. Jarosite from the supratidal zone displayed mean elemental ratios for K:Fe:S of 0.79:3:2.17 (n=26), which is relatively close to the ideal stoichiometry of 1:3:2. However, whilst molar ratios of Fe to S remained stable in the natural jarosite along the toposequence, Fe to K ratios indicated increasing depletion of K downslope with tidal inundation (Figure 3b). This depletion was strongly correlated with elevation (Figure 3a). These data are consistent with the findings of Smith *et al*. (2006), who demonstrated selective loss of K relative to Fe during dissolution of jarosite. Other studies have also reported incongruent dissolution of jarosite and retention of Fe relative to K (e.g. Jones *et al.* 2006; Welch *et al.* 2008).

Conclusion

Direct evidence from scanning electron microscopy (SEM) and x-ray diffractometry (XRD) identified jarosite in the former sulfuric horizon of tidally inundated ASS. Under reducing soil conditions, natural jarosite from the intertidal zone exhibited features consistent with dissolution. Molar ratios of Fe to K indicated increasing depletion of K in natural jarosite downslope. Results provide important insights to the observed and predicted variability and stability of jarosite with tidal inundation.

References

Brophy GP, Sheridan MF (1965) Sulfate studies IV: the jarosite-natrojarosite-hydronium jarosite solid solution series. *American Mineralogist* **50**, 1595-1607.

Dent D (1986) 'Acid sulphate soils: a baseline for research and development.' (International Institute for Land Reclamation and Improvement (ILRI): Wageningen, The Netherlands).

Dutrizac JE (1983) Factors affecting alkali jarosite precipitation. *Metallurgical Transactions B: Process Metallurgy* **14B**, 531-539.

Gasharova B, Göttlicher J, Becker U (2005) Dissolution at the surface of jarosite: an in situ AFM study. *Chemical Geology* **215**, 499-516.

Johnston SG, Bush RT*, et al.* (2009a) Changes in water quality following tidal inundation of coastal lowland acid sulfate soil landscapes. *Estuarine Coastal and Shelf Science* **81**, 257-266.

Johnston SG, Keene AF, Bush RT, Burton ED, Sullivan LA, Smith D, McElnea AE, Martens MA, Wilbraharn S (2009b) Contemporary pedogenesis of severely degraded tropical acid sulfate soils after introduction of regular tidal inundation. *Geoderma* **149**, 335-346.

Jones EJP, Nadeau T, Voytek MA, Landa ER (2006) Role of microbial iron reduction in the dissolution of iron hydroxysulfate minerals. *Journal of Geophysical Research* **111**, G01012.

Powell B, Martens M (2005) A review of acid sulfate soil impacts, actions and policies that impact on water quality in Great Barrier Reef catchments, including a case study on remediation at East Trinity. *Marine Pollution Bulletin* **51**, 149-164.

Smith AML, Hudson-Edwards KA, Dubbin WE, Wright K (2006) Dissolution of jarosite [KFe3(SO4)(2)(OH)(6)] at pH 2 and 8: Insights from batch experiments and computational modelling. *Geochimica et Cosmochimica Acta* **70**, 608-621.

van Breemen N (1973) Soil forming processes in acid sulphate soils. In 'Proceedings of the international symposium on acid sulphate soils'. (Ed. H Dost) pp. 66-129. (International Institute for Land Reclamation and Improvement: Wageningen, The Netherlands).

van Breemen N, Harmsen K (1975) Translocations of iron in acid sulfate soils: I. Soil morphology, and the chemistry and mineralogy of iron in a chronosequence of acid sulfate soils. *Soil Science Society of America Proceedings* **39**, 1140-1148.

Welch SA, Kirste D, Christy AG, Beavis FR, Beavis SG (2008) Jarosite dissolution II-Reaction kinetics, stoichiometry and acid flux. *Chemical Geology* **254**, 73-86.